THE JOURNAL OF BIOLOGICAL CHEMISTRY VOL. 281, NO. 50, pp. 38507–38518, December 15, 2006

The NH_2-terminal Propeptide of Type I Procollagen Acts Intracellularly to Modulate Cell Function*

Received for publication, August 8, 2006, and in revised form, September 25, 2006 Published, JBC Papers in Press, October 3, 2006, DOI 10.1074/jbc.M607536200

Anush Oganesian[‡], Sandra Au[‡], Jeremy A. Horst[‡], Lars C. Holzhausen[‡], Athena J. Macy[‡], James M. Pace[§], and Paul Bornstein[‡¶1]

From the Departments of [‡]Biochemistry, [¶]Medicine, and [§]Pathology, University of Washington, Seattle, Washington 98195

The function of the NH_2-terminal propeptide of type I procollagen (N-propeptide) is poorly understood. We now show that a recombinant trimeric N-propeptide interacts with transforming growth factor-β1 and BMP2 and exhibits functional effects in stably transfected cells. The synthesis of N-propeptide by COS-7 cells results in an increase in phosphorylation of Akt and Smad3 and is associated with a marked reduction in type I procollagen synthesis and impairment in adhesion. In C2C12 cells, N-propeptide inhibits the osteoblastic differentiation induced by BMP2. Our data suggest that these effects are mediated by the interaction of N-propeptide with an intracellular receptor in the secretory pathway, because they are not observed when recombinant N-propeptide is added to the culture medium of either COS-7 or C2C12 cells. Both the binding of N-propeptide to cytokines and its functional properties are entirely dependent on the exon 2-encoded globular domain, and a mutation that substitutes a serine for a highly conserved cysteine in exon 2 abolishes its function. Our findings suggest that N-propeptide performs an important feedback regulatory function and provides a rationale for the prominence of a homotrimeric form of type I procollagen (α1 trimer) during vertebrate development.

Fibrillar types I–III procollagens are proteolytically cleaved by procollagen N- and C-proteases that separate nontriple helical NH_2- and COOH-terminal propeptides, respectively, from their major central triple helical domains (1). This proteolytic processing is necessary for the alignment and self-assembly of collagen molecules and for normal collagen fibril formation. Specific sequences in the COOH-terminal propeptides are required for chain recognition and triple helix formation that generate procollagens with the correct chain composition (2–4). In addition, the COOH-terminal propeptide has been shown to be chemotactic for endothelial cells and to stimulate migration and production of metalloproteinases by mammary carcinoma cell lines after its release by procollagen C protease (5, 6). Fragments of the propeptide have also been reported to stimulate extracellular matrix production (7).

In contrast, the functions of the NH_2-terminal propeptide of type I procollagen (N-propeptide)[2] are not well understood (for a review see Ref. 8). In 1979, Wiestner *et al.* (9) purified the N-propeptide from dermatosparactic calf skin, which is deficient in procollagen N-protease, and demonstrated that it functioned to inhibit the synthesis of both types I and III collagen by bovine skin fibroblasts in culture. Subsequently, evidence was provided for the ability of the N-propeptide to inhibit selectively the translation of procollagen mRNA in cell-free systems (10, 11). However, this function, which presumes a cytosolic site of action, was never reconciled with the fact that the N-propeptide is released only in intracellular secretory vesicles and in the extracellular environment (12). Additional functions proposed for the N-propeptide included inhibition of intracellular fibrillogenesis, facilitation of transcellular transport and secretion of procollagen, and control of extracellular fibrillogenesis (for reviews see Refs. 8, 13, and 14), but none of these functions were supported by the phenotype of a mouse with a targeted deletion of exon 2 in the *Col1a1* gene. Thus, although exon 2 encodes the majority of the nontriple helical sequence in the N-propeptide, procollagen synthesis, secretion, and proteolytic processing were all normal in these mice (15). Excisional skin wound healing was also normal. However, a background-dependent reduction in the expected number of viable homozygous mutant mice that were born in heterozygous crosses was documented.

Because compensation by the closely related N-propeptide of type III procollagen, which is synthesized in a very similar spatial and temporal pattern to that of type I procollagen, seemed likely, we determined the levels of proα1(III) mRNA in exon 2-deleted mice. Extensive Northern analyzes of tissues from both pre- and postnatal mice of several ages revealed no differences from controls.[3] However, the possibility remains that normal levels of type III N-propeptide could compensate for a lack of type I N-propeptide. In addition, type V procollagen contains a cysteine-rich domain (CRD) in the proα2 chain of its NH_2-terminal propeptide that is homologous to N-propeptide.

* This work was supported by National Institutes of Health Grant R01 AR 11248 and by National Science Foundation Grant EEC 95291161. The costs of publication of this article were defrayed in part by the payment of page charges. This article must therefore be hereby marked "*advertisement*" in accordance with 18 U.S.C. Section 1734 solely to indicate this fact.

[1] To whom correspondence should be addressed: Dept. of Biochemistry, Box 357350, University of Washington, Seattle WA 98195. Tel.: 206-543-1789; Fax: 206-685-4426; E-mail: bornsten@u.washington.edu.

[2] The abbreviations used are: N-propeptide, NH_2-terminal propeptide of type I procollagen; AP, alkaline phosphatase; BMP, bone morphogenetic protein; CRD, cysteine-rich domain; HEK, human embryonic kidney; OI, osteogenesis imperfecta; TGF, transforming growth factor; ELISA, enzyme-linked immunosorbent assay; PBS, phosphate-buffered saline; DMEM, Dulbecco's modified Eagle's medium; FBS, fetal bovine serum; CICP, COOH-terminal propeptide of human type I procollagen; PI, phosphatidylinositol; PDGF, platelet-derived growth factor; PI3K, phosphatidylinositol 3-kinase.

[3] M. L. Augustine and P. Bornstein, unpublished results.

Type V procollagen is frequently co-expressed with type I procollagen and might therefore also compensate.

We then considered the possibility that N-propeptide might not function directly in collagen biogenesis but might rather play a developmental role by interaction with cytokines such as members of the TGFβ and BMP families. This possibility is supported by the presence of a CRD in the sequences encoded by exon 2 in types I–III procollagens that is homologous with the CRDs in chordins in vertebrates and sog in *Drosophila* (16). Chordin and sog bind BMPs in vertebrates and *Drosophila*, respectively, and function to regulate dorsoventral patterning during embryonic development (17–20). Larrain *et al.* (19) also showed that the N-propeptide derived from *Xenopus* type IIA procollagen bound BMP4 and that *Xenopus* type IIA procollagen mRNA had dorsalizing activity when microinjected into *Xenopus* embryos. These studies are supported by the work of Sandell and co-workers (21) who demonstrated that the N-propeptide of human type IIA procollagen, which contains the CRD sequence, but not the N-propeptide of type IIB procollagen, a splice variant that lacks the sequence encoded by exon 2, binds BMP2 and TGFβ1. In contrast with the mild phenotype of type I procollagen exon 2-deleted mice, mice with a targeted deletion of exon 2 in type II procollagen were found to die in mid-gestation because of cardiac malformations (22). This disparity is not necessarily surprising in view of the very different spatial and temporal patterns of expression of the two procollagens. Thus, the functional significance of their N-propeptides is almost certain to be very different even though their structures and intrinsic mechanisms of action may have similarities.

In this study we show that a recombinant trimeric N-propeptide interacts with both TGFβ1 and BMP2. N-propeptide also functions intracellularly, because COS-7 cells that are stably transfected with a cDNA encoding a trimeric form of the N-propeptide show an increase in the phosphorylation of Akt and Smad3, markedly reduce collagen synthesis, and attach poorly to fibronectin-coated plates. Furthermore, the expression of N-propeptide in stably transfected myoblastic C2C12 cells inhibits BMP2-induced differentiation to osteoblasts. These effects cannot be reproduced by addition of purified N-propeptide, or the conditioned medium of N-propeptide-expressing cells, to control COS-7 cells. All activities of N-propeptide can be attributed to the CRD encoded by exon 2, because a protein that lacks this sequence is defective in both functional and direct binding assays. The importance of a native structure of the CRD is highlighted by the finding that a recombinant mouse N-propeptide with a substitution of a serine for a cysteine, patterned after a naturally occurring mutation in a patient with osteogenesis imperfecta (OI), failed to signal appropriately in stably transfected COS-7 cells.

EXPERIMENTAL PROCEDURES

Construction of Mammalian Expression Vectors—The cDNA encoding the N-propeptide of type I procollagen, and an additional 111 amino acids from the major triple helix of the α1(I) chain, was excised from a full-length murine *Col1a1* cDNA and cloned in-frame with the DNA encoding a 27-amino acid foldon sequence derived from bacteriophage T4 fibritin protein (23). The resulting fusion sequence was amplified using primers designed to include an XbaI restriction site and a Kozak consensus translational start sequence at the 5′-end and a BstBI/SfuI site with a GSGS spacer at the 3′-end. The sequence was then cloned into a pcDNA3.1/Myc-His(+)B mammalian expression vector (Invitrogen). Preservation of the correct reading frame was verified by DNA sequencing. To prepare an N-propeptide construct lacking the amino acids encoded by exon 2, we used the above-described N-propeptide-containing plasmid as a template and a standard site-directed mutagenesis procedure with custom-designed primers to exclude the exon 2 sequence. The resultant PCR-amplified fragment was digested with XbaI and BstBI/SfuI enzymes and cloned into a pcDNA3.1/Myc-His(+)B plasmid. The structures of the two peptide fragments are illustrated schematically in Fig. 1. We also used a QuickChange II site-directed mutagenesis kit (Stratagene, La Jolla, CA) to create a G to C nucleotide mutation in the N-propeptide construct that resulted in the substitution of a serine for a cysteine at position 52 in the N-propeptide sequence (C52S mutant construct).

DNA Transfections—COS-7 and HEK293 cells (American Type Culture Collection, Manassas, VA) and C2C12 cells, a gift from Dr. S. Hauschka (University of Washington), were transfected with the two constructs described in Fig. 1, or with a control vector, using the Superfect transfection reagent (Qiagen Inc., Valencia, CA). In addition, COS-7 cells were transfected with the C52S mutant construct. To establish stably transfected cell lines for each protein, cells were selected with G418 (COS-7, 400 μg/ml; HEK293, 500 μg/ml; and C2C12, 700 μg/ml) for 2 weeks, followed by expansion of isolated clones. Multiple clones were evaluated for protein expression levels by Western blotting with c-Myc antibody (Santa Cruz Biotechnology, Santa Cruz, CA) and monospecific anti-mouse N-propeptide rabbit polyclonal antibody (prepared in our laboratory). To determine transfection efficiency, some plates were co-transfected with the reporter vector pEGFP-C3 (Clontech).

Protein Purification—Individual clones expressing intact N-propeptide, exon 2-deleted N-propeptide, or the C52S mutant were grown to confluence in DMEM (Invitrogen) with 10% FBS. Cells were serum-starved for 24 or 48 h, the medium was collected, and the proteins were purified using nickel-nitrilotriacetic acid HisBind resins (Novagen, Madison, WI). The purity of the proteins was determined by silver staining using a Silver Stain Plus kit (Bio-Rad).

Western Blotting—Proteins were separated by SDS-PAGE and transferred to nitrocellulose membranes. The membranes were blocked at room temperature for 1 h with 5% nonfat dry milk in TBST (Tris-buffered saline containing 0.1% Tween 20). The blots were incubated with primary antibodies at 4 °C overnight, washed four times with TBST, and incubated for 40 min with secondary anti-rabbit or anti-mouse antibodies, conjugated with horseradish peroxidase (Amersham Biosciences). The immunoreactive protein bands were visualized using a chemiluminescence (ECL) detection system (Amersham Biosciences).

Determination of N-propeptide Concentrations by ELISA—96-Well ELISA plates (Corning Glass) were coated overnight at 4 °C with 100 μl of serum-deprived conditioned medium from control COS-7 cells or cells expressing one of the three

N-propeptides. Plates were washed four times with the PBS, 0.1% Tween 20 (Fisher) and blocked with PBS, 1% bovine serum albumin (Sigma) for 1 h at room temperature. An anti-Myc antibody was added to each well and incubated for 2 h at room temperature. Plates were washed, blocked again, and incubated with anti-mouse AP-conjugated secondary antibody for 1 h at room temperature. *p*-Nitrophenyl phosphate liquid solution (Sigma) was used as a substrate, and absorbance was measured at 405 nm.

Cell Attachment and Detachment Assays—COS-7 cells, transfected with N-propeptide or exon 2-deleted N-propeptide, and control COS-7 cells were trypsinized, and 100 μl of a cell suspension (10^4 cells) was added to each well of fibronectin-coated, 96-well tissue culture plates. Cells were allowed to attach for 1 h at 37 °C. Unattached cells were removed by washing the plates with PBS, and attachment was quantified by addition of 20 μl of Cell Titer 96 solution, according to the manufacturer's instructions (Promega, Madison, WI.). After 1 h of incubation at 37 °C, the absorbance at 490 nm was measured in a microplate reader. To quantify the rate of detachment, control COS-7 cells and cells stably expressing either N-propeptide or exon 2-deleted N-propeptide were trypsinized and plated in triplicate in 12-well plates at a density of 6×10^4 cells per well. The cells were grown to 80% confluence, washed twice with PBS, and treated with 0.05% trypsin, and detached cells were counted at different time points. The percentage of detached cells was calculated by dividing the number of detached cells by the number of cells introduced in each well.

ELISA for Collagen Synthesis—Control COS-7 cells and N-propeptide or exon 2-deleted N-propeptide-expressing cells were plated and cultured in DMEM with 10% FBS. When cells reached 80–90% confluence, the culture medium was removed, and the cells were washed twice with PBS and cultured in serum-free medium for an additional 6 or 24 h. This culture medium was then collected and immediately stored at −80 °C for use in ELISAs. The cell number in each dish was then counted to determine the quantity of cells that had contributed to the generation of type I collagen that was secreted into the medium over the 24-h period. ELISA was performed in duplicate using a Metra CICP EIA kit (Metra Biosystems, San Diego). Briefly, aliquots of media from control COS-7 cells and from cells expressing N-propeptide or exon 2-deleted N-propeptide were added to 8-well strips coated with a monoclonal antibody to the COOH-terminal propeptide of human type I procollagen (CICP) and incubated for 2 h at room temperature. This antibody cross-reacts with the monkey procollagen synthesized by COS-7 cells. Wells were washed and incubated with rabbit anti-CICP polyclonal antibody followed by incubation with a goat anti-rabbit AP conjugate. *para*-Nitrophenyl phosphate substrate was used to quantify CICP in the medium. The results were converted to nanograms/ml using standards provided by the manufacturer and normalized according to the number of cells present at the time of medium collection.

Immunoprecipitation of TGFβ1 and BMP2—100 μl of cell culture medium containing N-propeptide or exon 2-deleted N-propeptide was incubated for 2 h at 37 °C with a 10–50-fold molar excess of TGFβ1 (PeproTech, Rocky Hill, NJ) or BMP2 (Wyeth, Cambridge, MA). Five μl of an anti-TGFβ1 polyclonal antibody (Promega, Madison, WI), or in the case of BMP2-containing tubes our monospecific anti-mouse N-propeptide polyclonal antibody, was then added to the appropriate tubes, and the solutions were incubated overnight at 4 °C. As negative controls, the conditioned medium from COS-7 cells, or from cells transfected with control plasmid only, was used. 30 μl of protein A/G-Sepharose was added, and the beads were incubated for 3 h at 4 °C. The beads were pelleted, washed four times with PBS containing 0.1% Triton 100, and once with 10 mM Tris, pH 6.8. The beads were then boiled in SDS sample buffer, and the supernatant was electrophoresed in SDS-acrylamide gels, electroblotted onto nitrocellulose membranes, and probed with monoclonal antibodies to c-Myc in the case of TGFβ1-containing samples or to BMP2 (Sigma) in the case of BMP2-containing samples.

Determination of the Levels of Phosphorylated Akt and Smad Proteins in COS-7, HEK293, and C2C12 Cells—Control COS-7 or human embryonic kidney HEK293 cells, transfected with an N-propeptide or exon 2-deleted N-propeptide plasmid, were serum-starved for 24 h. Mouse myoblast C2C12 cells were kept in 2% serum overnight. Control cells were treated with 5 ng/ml TGFβ1 or 100 ng/ml BMP2 for 1 h. Cells were washed twice with PBS and lysed in 1% Nonidet P-40 buffer (1% Nonidet P-40, 120 mM NaCl, 50 mM Tris-HCl, pH 7.4, protease inhibitor mixture, 20 mM NaF, and 1 mM Na_3VO_4) on ice for 20 min. Cell lysates were clarified by centrifugation at 14,000 rpm at 4 °C for 20 min, and protein concentrations were then determined by the BCA method (Pierce). 30-μg aliquots of total cell lysates were separated by SDS-PAGE and transferred to nitrocellulose membranes. Western blot analyses were performed using phospho-Akt, pan-Akt, phospho-Smad2, phospho-Smad3, total Smad2/3, phospho-Smad 1/5/8 (Cell Signaling Technology, Beverly, MA), and anti-β-actin (Novus Biologicals, Littleton, CO) antibodies, as described above.

When TGFβRI kinase inhibitor (Calbiochem) was used, control COS-7 cells or cells expressing N-propeptide were serum-starved, and different concentrations of inhibitor (4, 8, and 18 nM) were added for 1 h prior to the addition of recombinant TGFβ1 or PDGF-BB to control cells. The cells were incubated for 10 min with PDGF-BB or 1 h with TGFβ1. N-propeptide-expressing cells were incubated with inhibitor for 1 or 4 h or overnight. Cells were washed with cold PBS, lysed, and analyzed by Western blotting as described above.

Apoptosis Assay—Control COS-7 cells and cells expressing N-propeptide or exon 2-deleted N-propeptide were serum-starved for 24 h and labeled with commercially available annexin V-PE (phycoerythrin) for assay of apoptosis (BD Biosciences) according to the manufacturer's recommendations. Briefly, 1×10^5 cells were washed twice with cold PBS, trypsinized, and resuspended in 100 μl of 1× binding buffer. Five μl of annexin V-PE was added, and the cells were incubated in the dark for 15 min and then analyzed by flow cytometry.

Determination of AP Activity in C2C12 Cells—C2C12 cells were cultured in DMEM containing 15% FBS, 100 units/ml penicillin, and 100 μg/ml streptomycin at 37 °C in a humidified atmosphere of 5% CO_2. Cells were stably transfected with the constructs shown in Fig. 1. Single clones were isolated and expanded as described above. To determine AP activity, the

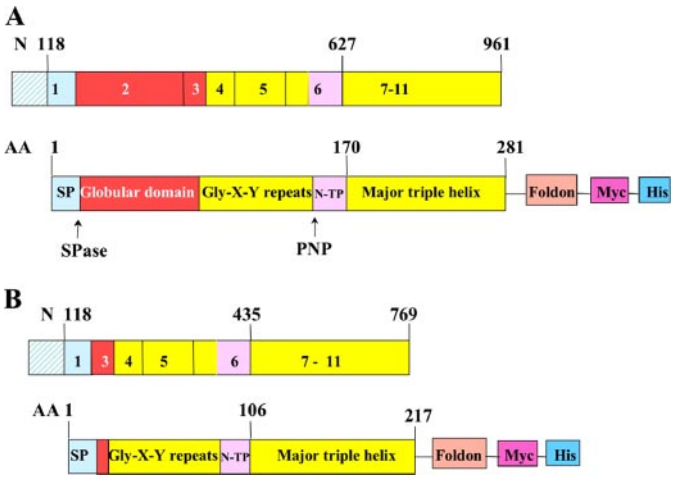

FIGURE 1. **Schematic representation of the proteins used in functional studies of the N-propeptide.** *A,* exons in the *Col1a1* gene and protein domains in an N-propeptide-foldon construct that was used to express the intact, trimeric mouse N-propeptide are shown. The sequence contains a signal peptide (*SP*, *light blue*), a globular domain encoded by exons 2 and 3 (*red*), a short triple helix (Gly-*X*-*Y* repeats) encoded by exons 4–6 (*yellow*), a short sequence that represents the site of cleavage by procollagen N-protease (*PNP*), an NH_2-terminal telopeptide sequence (*N-TP, mauve*), 111 amino acids of the major triple helix encoded by exons 7–11, a 27-amino acid foldon trimerizing domain, a Myc tag for Western blotting, and a His tag for column purification. *B,* exons and structure of a trimeric N-propeptide that lacks most of the globular domain encoded by exon 2 but is identical in all other respects to the structure of the trimeric N-propeptide shown in *A*.

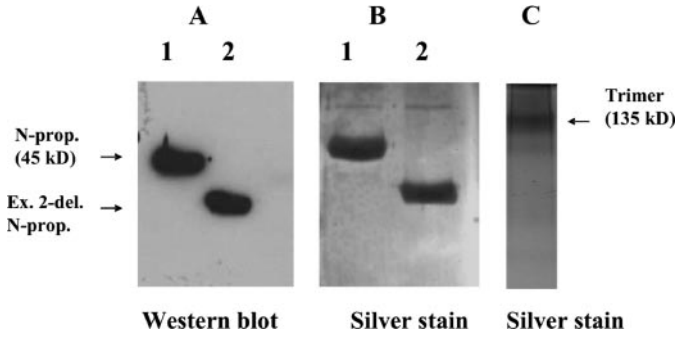

FIGURE 2. **Analysis of N-propeptide-foldon fusion proteins.** Proteins produced by stably transfected COS-7 cells were purified from conditioned medium by nickel affinity chromatography. *A,* Western blot analysis with anti-Myc antibody of conditioned medium from COS-7 cells stably expressing N-propeptide (*N-prop.*; *lane 1*) or exon 2-deleted N-propeptide (*Ex.2-del. N-prop.*; *lane 2*) electrophoresed in SDS gels under reducing conditions. *B,* silver-stained SDS-acrylamide gel of purified N-propeptide (*lane 1*) or exon 2-deleted N-propeptide (*lane 2*) run as described in *A*. *C,* silver-stained gel of purified N-propeptide run in absence of SDS and reducing agents.

cells were plated at 4×10^4 cells/well in 24-well tissue culture plates. Following a 24-h incubation period, the cells were rinsed with PBS, and growth medium was replaced with DMEM containing 2% FBS and 50 ng/ml BMP2 (Wyeth) and the cells were incubated for another 3 days. Cells were washed twice with cold PBS and lysed in a buffer containing 50 mM Tris-HCl, 75 mM NaCl, and 0.5% Triton-100 at pH 7.5. The cellular AP activity, a prominent osteoblastic differentiation marker, was determined in cell lysates in a buffer containing 0.1 M 2-amino-2-methyl-1-propanol (Sigma), pH 10.5, and *p*-nitrophenyl phosphate (Sigma) as a substrate. Absorbance was recorded at 405 nM. Determination of the AP activity was performed in triplicate, and the values were normalized to total protein concentrations using a BCA assay kit (Pierce).

Statistical Analysis—A two-tailed Student *t* test was used for statistical comparisons. Data were considered statistically significant when the *p* value was less than 0.05.

RESULTS

Purification of N-propeptide-Foldon Fusion Proteins—To study the biochemical function of the N-propeptide of type I procollagen, a chimeric gene construct, consisting of cDNA encoding the full-length N-propeptide, and an additional 111 amino acids from the major triple helix of the α1(I) chain, was generated recombinantly. These sequences were fused to a foldon sequence from T4 bacteriophage fibritin that is known to have strong trimerizing properties (Fig. 1*A*). The rationale for construction of a trimeric N-propeptide is provided under the "Discussion." The additional 37 Gly-*X*-*Y*- triplet sequences were placed NH_2-terminal to the foldon sequence to generate a relatively stable triple helix that would fold from the COOH to the NH_2 terminus (23), and thus make it more likely that the orientation of the three globular domains in the trimeric N-propeptide resembled that in the native protein. To evaluate whether the exon 2-encoded CRD is responsible for the biological function of the N-propeptide, we deleted the exon 2 sequence from the above construct. The structure of the resulting fusion protein is shown schematically in Fig. 1*B*. We also studied the effect of substitution of a serine for a cysteine, a naturally occurring mutation at amino acid 61 (C61S) of the proα1 chain of type I procollagen in a patient with OI.[4] A point mutation was created that changed a Cys to a Ser in the corresponding position (amino acid 52) of the mouse N-propeptide construct.

COS-7, HEK293, and C2C12 cells were stably transfected with the N-propeptide, and exon 2-deleted N-propeptide constructs and expression levels of the encoded proteins were evaluated in isolated clones by Western blots of the conditioned media with c-Myc antibody. COS-7 cells were also transfected with the C52S mutant N-propeptide. Expression levels of three recombinant proteins were comparable (data not shown). Conditioned medium from clones with high expression levels, as determined by Western blot with c-Myc antibody (Fig. 2*A*), was used to purify recombinant proteins by nickel affinity chromatography. As shown in Fig. 2*B*, silver staining of SDS-acrylamide gels indicated that the purified proteins were homogeneous and free of contaminating proteins. A similar degree of purity was achieved for the mutant N-propeptide (data not shown). In the absence of denaturing agents (native gels), intact trimeric N-propeptide migrates to a position consistent with its molecular weight (Fig. 2*C*). The amount of each recombinant protein present in conditioned medium was quantified using an ELISA-based assay, as described under "Experimental Procedures," and used as a basis for comparison in subsequent experiments. The three proteins were present at approximately equal levels (200–300 ng/ml).

The Expression of N-propeptide Compromises Attachment and Accelerates Detachment of COS-7 Cells—During culture of stably transfected COS-7 cells, it was noticed that cells that

[4] J. M. Pace and P. H. Byers, unpublished data.

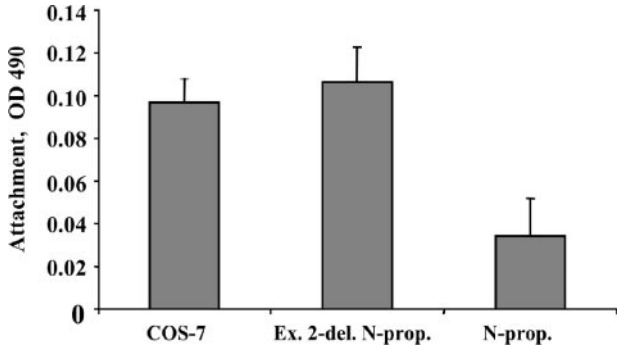

FIGURE 3. **Expression of N-propeptide reduces the attachment of COS-7 cells.** Control COS-7 cells, cells stably transfected with exon 2-deleted N-propeptide (*Ex.2-del. N-prop.*) or with N-propeptide (*N-prop.*) were trypsinized, and 10^4 cells were plated onto 96-well plates coated with fibronectin. Cells were allowed to attach for 1 h; nonadherent cells were removed, and attachment was quantified by addition of 20 μl of Cell Titer 96 solution. Data represent mean values ± S.D. of triplicate determinations. This experiment was repeated three times with similar results.

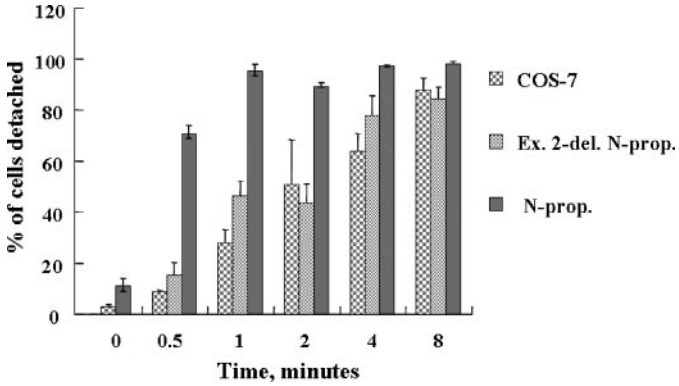

FIGURE 4. **Detachment of COS-7 cells is accelerated in N-propeptide-expressing cells.** Control COS-7 cells, cells stably transfected with exon 2-deleted N-propeptide (*Ex.2-del. N-prop.*) or cells transfected with N-propeptide (*N-prop.*), were plated in triplicate in 12-well tissue culture plates at 6×10^4 cells per well. Cells were grown to 80% confluence and trypsinized with 0.05% trypsin at the indicated time points, and detached cells were counted. Data represent mean values ± S.D. of triplicate determinations. The experiment was performed twice with similar results.

secreted N-propeptide appeared to attach more slowly, as compared with exon 2-deleted or mutant N-propeptide, when plated and to detach more rapidly when passaged. We therefore proceeded to document these changes. Control COS-7 cells or COS-7 cells stably expressing either N-propeptide or exon 2-deleted N-propeptide were cultured on fibronectin-coated plates for 1 h. The unattached cells were removed, and the attachment of cells was quantified as described under "Experimental Procedures." The results demonstrate that the rate of attachment of COS-7 cells expressing exon 2-deleted N-propeptide was comparable with that of control COS-7 cells (Fig. 3). In contrast, the rate of attachment of COS-7 cells expressing N-propeptide was reduced by ~70%, compared with that of control cells or of cells expressing exon 2-deleted N-propeptide. These data demonstrate that the synthesis and secretion of N-propeptide compromised the ability of COS-7 cells to attach to a substratum.

COS-7 cells expressing N-propeptide also detached more rapidly than control or exon 2-deleted cells when exposed to low concentrations of trypsin. The results presented in Fig. 4 demonstrate that a 30-s treatment with 0.05% trypsin resulted in detachment of greater than 70% of COS-7 cells expressing N-propeptide, and a 60-s incubation leads to almost 100% detachment of the cells. In contrast, only 10–20 and 30–50% of control or exon 2-deleted N-propeptide-expressing COS-7 cells were detached at the same time points. These data confirm that the expression of N-propeptide leads to an acceleration of the detachment of COS-7 cells when these cells are subjected to mild proteolysis. In the case of both reduced attachment and accelerated detachment, the cause can be attributed to the CRD domain encoded by exon 2. In contrast, no differences in the attachment or detachment of HEK293 or C2C12 cells, expressing N-propeptide or exon 2-deleted N-propeptide, were observed in comparison with the respective control cells. Also, no differences in the attachment or detachment of COS-7 cells expressing C52S mutant N-propeptide were observed (data not shown).

Collagen Synthesis Is Reduced in COS-7 Cells That Stably Express N-propeptide—In view of earlier studies that implicated N-propeptide in feedback inhibition of collagen synthesis (9), we chose to examine the synthesis and secretion of type I procollagen by COS-7 cells. COS-7 cells are SV40-transformed monkey kidney fibroblast-like cells. These cells are closely related to COS-1 cells, which normally produce small but measurable amounts of type I collagen (24). We therefore determined the amount of type I procollagen produced *de novo* and secreted into the culture medium over a 24-h time period by control COS-7 cells and by COS-7 cells expressing either N-propeptide or exon 2-deleted N-propeptide. The amount of type I procollagen found in media harvested from control COS-7 cells, as determined by ELISA using a monoclonal antibody to the COOH terminus of human type I procollagen, was 29.5 ng/ml, whereas the level in N-propeptide-expressing cells was 6.5 ng/ml (Table 1). The level of type I procollagen in COS-7 cells expressing exon 2-deleted N-propeptide was comparable with that in control cells. Similar differences in the levels of procollagen in the media of these cells were seen at a 6-h time point (data not shown), making it unlikely that procollagen was preferentially incorporated into the cell layer of N-propeptide-expressing cells as a function of time. These data indicate that the expression of N-propeptide by COS-7 cells results in a 4–5-fold reduction in the amount of type I collagen produced by these cells and that again the exon 2-encoded sequence is required for this effect. Reduced deposition of type I collagen, and possibly other matrix proteins, in the subcellular stratum of N-propeptide-producing cells could contribute to the adhesive defect in these cells.

N-propeptide Interacts Directly with TGFβ1 and BMP2—It is well known that TGFβ1 functions as a major fibrogenic cytokine that stimulates the production of fibrous collagens, fibronectin, and proteoglycans by mesenchymal cells (25, 26). Furthermore, the N-propeptide of type II procollagen has been shown to be capable of binding to TGFβ1 (21). Because the CRD domains encoded by exon 2 in types I and II procollagens show a high degree of sequence identity (8), it seemed logical to determine whether N-propeptide could also bind to TGFβ1. Toward this end, we performed direct immunoprecipitation assays with an anti-TGFβ1 antibody. COS-7 cells, stably

TABLE 1
Secreted type I procollagen levels in COS-7 cells
Values are presented as means ± S.E. ($n = 3$).

	Type I procollagen	Type I procollagen levels
	ng/ml	*%*
Control COS-7 cells	29.52 ± 1.30	100
COS-7 cells expressing exon 2-deleted N-propeptide	32.24 ± 7.64	109
COS-7 cells expressing N-propeptide	6.50 ± 0.50[a]	22

[a] $p < 0.005$ compared with control COS-7 cells.

expressing N-propeptide or exon 2-deleted N-propeptide, were serum-starved for 24 h. Equal quantities of TGFβ1 were then added to aliquots of conditioned medium, and the solutions were incubated for 2 h at 37 °C. A TGFβ1-specific antibody was used to immunoprecipitate putative TGFβ1-N-propeptide complexes. Western blot analysis with a c-Myc antibody revealed that N-propeptide co-precipitated with TGFβ1 (Fig. 5*A*, *lane 2*). On the other hand, incubations of TGFβ1 with conditioned medium from control COS-7 cells, exon 2-deleted N-propeptide-transfected cells, or vector-transfected COS-7 cells failed to show an interaction with N-propeptide (Fig. 5*A*, *lanes 1, 3,* and *4*). Similar results were obtained in immunoprecipitation assays performed with purified, recombinant N-propeptide and exon 2-deleted N-propeptide (data not shown). These results confirm that the interaction of N-propeptide with TGFβ1 requires the presence of the exon 2-encoded CRD domain.

BMPs, including BMP2, are involved in early development and in differentiation of tissues (27). In view of our previous finding of significant fetal mortality in mice that lacked exon 2 of the *Col1a1* gene, and the observation by Zhu *et al.* (21) that the closely related type II collagen N-propeptide was capable of binding BMP2, we tested the ability of N-propeptide to bind BMP2. As shown in Fig. 5*B*, anti-N-propeptide antibodies were capable of co-immunoprecipitating N-propeptide from the culture medium of COS-7 cells, stably transfected with a vector expressing N-propeptide (*lane 3*), but not from that of cells transfected with empty vector (*lane 2*). In a separate experiment using purified proteins, we showed that N-propeptide, but not exon-deleted N-propeptide, bound BMP2. In this case an anti-c-Myc antibody was used for immunoprecipitation (data not shown).

Endogenously Acting N-propeptide Increases the Phosphorylation of Akt and Smad3, but Not Smad2, in COS-7 Cells—It has been shown that both phosphatidylinositol 3-kinase (PI 3-kinase) and the PI 3-kinase-dependent serine-threonine kinase, Akt, can be activated by TGFβ1 in COS-7 cells (28). We therefore used COS-7 cell lines, stably expressing and secreting N-propeptide, to determine whether N-propeptide could interfere with the activation of Akt by binding to TGFβ1. Control COS-7 cells and stably transfected COS-7 cell lines were grown to 90% confluence and were serum-deprived for 24 h. Cells were stimulated with TGFβ1 for 1 h and lysed, and the levels of phospho-Akt (pAkt) were determined by Western blot analysis using a pAkt-specific antibody. However, it soon became apparent that the pAkt levels in N-propeptide-expressing cells were as high, or higher, than the levels in TGFβ1-stimulated

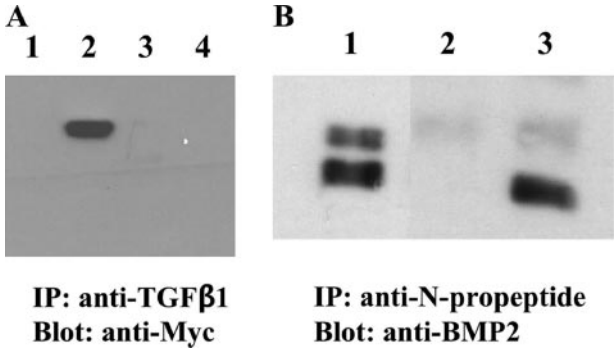

FIGURE 5. **Co-immunoprecipitation of N-propeptide with TGFβ1 and BMP2.** *A,* TGFβ1 was added to the conditioned media of different COS-7 cell lines. The media were then incubated for 2 h at 37 °C and immunoprecipitated (*IP*) with an anti-TGFβ1 antibody. The resultant immunoprecipitates were resolved on an SDS-acrylamide gel and blotted with an anti-Myc antibody to detect the N-propeptide fusion protein. *Lane 1,* control COS-7 cells; *lane 2,* COS-7 cells stably expressing N-propeptide; *lane 3,* COS-7 cells stably expressing exon 2-deleted N-propeptide; *lane 4,* COS-7 cells stably transfected with a control vector. *B,* BMP2 (100 ng) was added to conditioned media from COS-7 cells, stably transfected with a control vector (*lane 2*) or COS-7 cells stably expressing N-propeptide (*lane 3*). *Lane 1* represents standard BMP2. The media were then incubated for 3 h at 37 °C and immunoprecipitated with an anti-N-propeptide antibody. The resultant immunoprecipitates were resolved on an SDS-acrylamide gel and blotted with an anti-BMP2 antibody.

cells (see Fig. 7). Thus, as shown in Fig. 6*A*, basal levels of pAkt were markedly increased in N-propeptide-expressing cells (*lane 3*), in comparison with control cells (*lane 1*), or with cells expressing exon 2-deleted N-propeptide (*lane 2*). Of interest, COS-7 cells that expressed the C52S mutant N-propeptide failed to increase pAkt (Fig. 6*A*, *lane 4*).

To determine whether endogenously produced N-propeptide also increased the phosphorylation of Smad proteins, control COS-7 cells and stably transfected cells were analyzed by Western blotting for levels of phospho-Smad2 and phospho-Smad3. As shown in Fig. 6*B*, basal levels of pSmad3 were markedly increased in N-propeptide-expressing cells (*lane 3*), in comparison with control COS-7 cells (*lane 1*) or with cells expressing exon 2-deleted N-propeptide (*lane 2*); again this level exceeded that achieved by addition of TGFβ1 to control cells (data not shown). As in the case of pAkt, C52S mutant N-propeptide-expressing COS-7 cells resembled exon 2-deleted N-propeptide-expressing cells in being incapable of increasing the phosphorylation of Smad3 (Fig. 6*B*, *lane 4*). On the other hand, the level of phosphorylated Smad2 in these cells was undetectable (data not shown; see "Discussion").

Treatment of N-propeptide-expressing COS-7 cells with PI 3-kinase-specific inhibitor, LY294002 (20 μM), inhibited the phosphorylation of Akt but not the phosphorylation of Smad3 (Fig. 6*C*, *lane 5*), suggesting that Smad3 activation in N-propeptide expressing cells is not PI 3-kinase-dependent. In keeping with the lack of an effect of N-propeptide on the adhesion of HEK293 cells, the expression of N-propeptide did not change the levels of phosphorylated Smad3 and Akt in these cells (data not shown). The distinction in response to N-propeptide between COS-7 and HEK293 cells is consistent with the morphology of these cells; COS-7 cells are distinctly fibroblastic, whereas HEK293 cells are epithelioid in appearance.

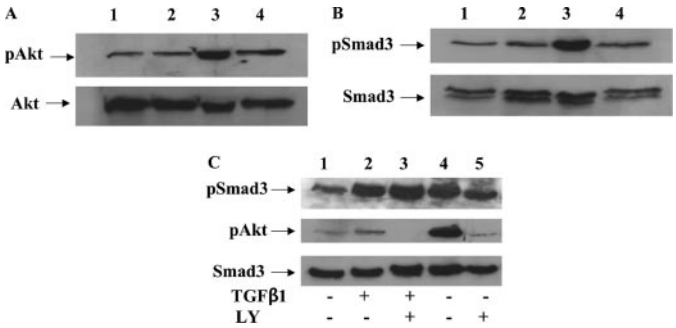

FIGURE 6. **Endogenously produced N-propeptide increases the phosphorylation of Akt and Smad3.** *A,* control COS-7 cells (*lane 1*) or cells stably transfected with exon 2-deleted N-propeptide (*lane 2*), with N-propeptide (*lane 3*), or with C52S mutant (*lane 4*) were serum-starved for 24 h and then lysed. Cell lysates were separated by SDS-PAGE and analyzed by Western blotting using p-Akt or pan-Akt antibodies. *B,* control COS-7 cells (*lane 1*), cells stably transfected with exon 2-deleted N-propeptide (*lane 2*), with N-propeptide (*lane 3*), or with C52S mutant (*lane 4*), were serum-starved for 24 h and lysed. Cell lysates were separated by SDS-PAGE and analyzed by Western blotting using phospho-Smad3 or total Smad3 antibodies. *C,* inhibition of PI3K/Akt pathway does not affect phosphorylation of Smad3. Control COS-7 cells (*lanes 1–3*) or cells stably transfected with N-propeptide (*lanes 4* and *5*) were serum-starved for 24 h and then treated with 10 ng/ml TGFβ1 for 1 h (*lanes 2* and *3*) and/or LY294002 (*LY*; *lanes 3* and *5*). Cell lysates were separated by SDS-PAGE and analyzed by Western blotting using p-Akt, p-Smad3, or Smad3 antibodies. This experiment is representative of three independent experiments.

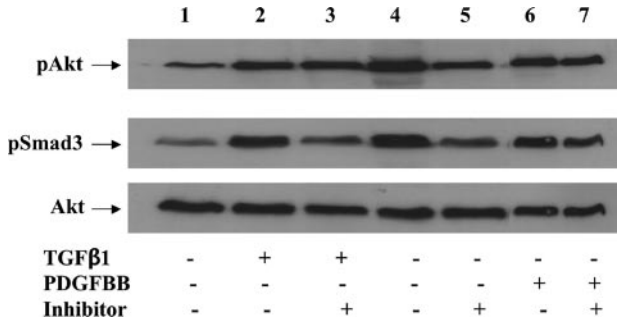

FIGURE 7. **TGFβRI kinase-specific inhibitor reduces phosphorylation of Smad3 in COS-7 cells.** Control COS-7 cells (*lanes 1–3, 6,* and *7*) and cells expressing N-propeptide (*lanes 4* and *5*) were treated with 8 nM TGFβR1 kinase inhibitor (*lanes 3, 5,* and *7*) followed by stimulation with 10 ng/ml TGFβ1 for 1 h (*lanes 2* and *3*) or with 50 ng/ml PDGF-BB for 10 min (*lanes 6* and *7*) as a control. Cells were lysed, and cell lysates were separated by SDS-PAGE and analyzed by Western blotting using phospho-Akt, phospho-Smad3, or pan-Akt antibodies. These experiments were repeated three times with similar results.

A TGFβRI Kinase-specific Inhibitor Reduces Phosphorylation of Smad3 in COS-7 Cells—Signaling by members of the TGFβ superfamily is mediated by two transmembrane receptor serine/threonine kinases, types I (TGFβRI) and II. Generally, ligand interaction with the type II receptor recruits and activates type I receptor. Activated TGFβRI then phosphorylates a subset of downstream signaling molecules, Smad proteins. To determine whether the high levels of pSmad3 or pAkt in N-propeptide-expressing COS-7 cells depend on the kinase activity of TGFβRI, we used different concentrations of a TGFβRI kinase-specific inhibitor and examined phosphorylation of Akt and Smad3 at different time points. As shown in Fig. 7, *lane 5*, the inhibitor reduced the level of pSmad3 in COS-7 cells expressing N-propeptide almost to the basal level; the level of pAkt was also reduced but to a somewhat higher level than that in control cells (Fig. 7, *lane 1*). As expected, TGFβ1 increased the phosphorylation of both Akt and Smad3 (Fig. 7, *lane 2*). To determine the specificity of the kinase inhibitor, we treated COS-7 cells with 50 ng/ml PDGF-BB for 10 min and examined phosphorylation of Akt and Smad3. As shown in Fig. 7 (*lanes 6* and *7*), pAkt and pSmad3 are also increased over control levels, but there is no difference in the extent of phosphorylation with or without the inhibitor. These data suggest that increased Smad3 phosphorylation in response to the expression of N-propeptide in these cells is due specifically to the activation of TGFβRI.

Endogenously Acting N-propeptide Inhibits BMP2-induced Osteoblastic Differentiation of C2C12 Cells—C2C12 myoblasts can be induced to differentiate into osteoblasts with BMP2. We therefore transfected C2C12 cells with N-propeptide and exon 2-deleted N-propeptide constructs and with control vector. We expanded single clones that stably expressed and secreted these proteins, and we examined the effect of BMP2 on their differentiation, as determined by the level of AP activity. We first determined that 50 ng/ml BMP2 is sufficient to differentiate control C2C12 cells into AP-positive osteoblast-like cells (data not shown). The ability of BMP2 to stimulate osteoblastic differentiation was reduced by ~70% in clones expressing N-propeptide, compared with that in control cells (Fig. 8*A*). Clones expressing exon 2-deleted N-propeptide failed to inhibit BMP2-induced differentiation and showed AP activity comparable with that of control cells.

To determine whether endogenously expressed N-propeptide also increased the phosphorylation of Akt or Smad proteins in C2C12 cells, control C2C12 cells expressing vector only and cells stably transfected with exon 2-deleted N-propeptide or with N-propeptide were analyzed by Western blotting using phosphorylated Akt- and Smad- specific antibodies. As shown in Fig. 8, *B* and *C*, the basal levels of pSmad3 or of pSmad1/5/8 in N-propeptide-expressing cells (*lane 3*) were not changed compared with cells expressing control vector (*lane 1*) or exon 2-deleted N-propeptide-expressing cells (*lane 2*). C2C12 cells are capable of responding to both TGFβ1 and BMP2 as shown in Fig. 8, *B* and *C* (*lane 4*). However, the level of p-Akt in N-propeptide-expressing cells (Fig. 8*D, lane 3*) was increased compared with those of controls (Fig. 8*D*, *lanes 1* and *2*). Addition of recombinant TGFβ1 did not increase the level of phosphorylated Akt in C2C12 cells (Fig. 8*D*, *lane 4*), suggesting that PI 3-kinase-dependent serine-threonine kinase, Akt, is not activated by TGFβ1 in these cells.

Externally Acting N-propeptide Is Incapable of Affecting the Phosphorylation Levels of Smad3 or Akt or the Synthetic or Differentiation Capability of Cells—To determine whether exogenous N-propeptide is also capable of stimulating the phosphorylation of Akt or Smad proteins, we cultured COS-7 cells in the presence of different concentrations of purified N-propeptide, ranging from 500 ng/ml to 10 μg/ml, and we examined the phosphorylation of Akt and Smads at different time points. The purified protein was added to the cells cultured either in serum-deprived conditions or in 10% serum. Equimolar amounts of recombinant exon 2-deleted N-propeptide were used as a negative control. Under these experimental conditions, no increase in the level of phosphorylation of Akt or Smad proteins was observed (data not shown). Similar results were obtained with

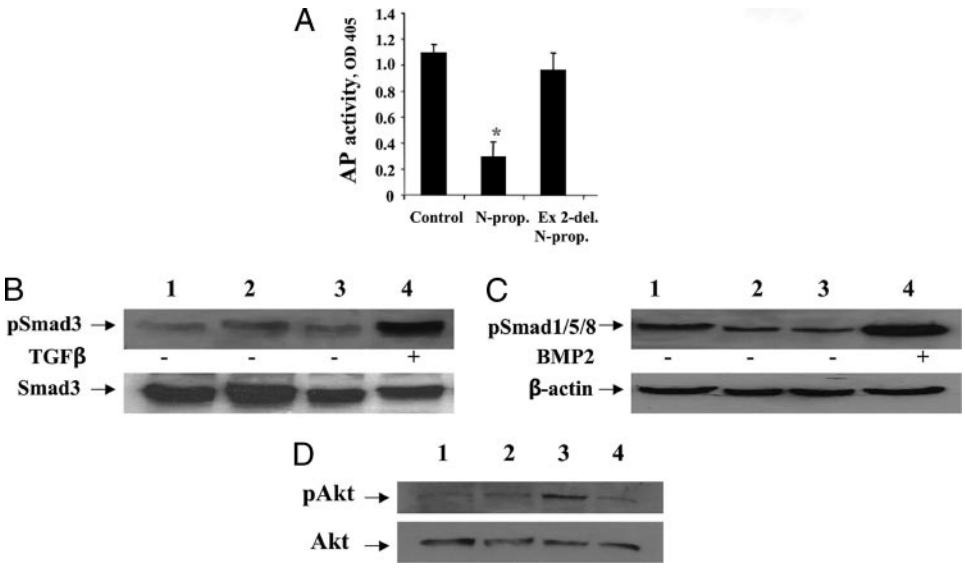

FIGURE 8. **Endogenously produced N-propeptide increases the phosphorylation of Akt and inhibits the function of BMP2.** *A,* control C2C12 cells, cells expressing N-propeptide (*N-prop.*) or exon 2-deleted N-propeptide (*Ex.2-del. N-prop.*) were cultured for 72 h in the presence of BMP2 (50 ng/ml). AP activity was then assayed in cell lysates. The results are averages of three individual experiments. *, $p \leq 0.0001$ for the difference between control and N-propeptide. *B* and *C,* expression of N-propeptide in C2C12 cells does not affect phosphorylation of Smad proteins. C2C12 cells, stably transfected with a control vector (*lanes 1* and *4*), with exon 2-deleted N-propeptide (*lane 2*) or with N-propeptide (*lane 3*) were cultured in 2% FBS containing medium for 24 h and then lysed. Cell lysates were separated by SDS-PAGE and analyzed by Western blotting using phospho-Smad3 or phospho-Smad1/5/8 antibodies. *Lane 4* represents control C2C12 cells treated with 5 ng/ml TGFβ1 (*B*) or with 100 ng/ml BMP2 (*C*) for 30 min. Membranes were stripped and probed with total Smad3 and β-actin antibodies for loading controls. *D,* expression of N-propeptide in C2C12 cells increases the phosphorylation of Akt. C2C12 cells stably transfected with a control vector (*lanes 1* and *4*), with exon 2-deleted N-propeptide (*lane 2*), or with N-propeptide (*lane 3*) were cultured in 2% FBS-containing medium for 24 h and then lysed. Cell lysates were separated by SDS-PAGE and analyzed by Western blotting using phospho-Akt. Membranes were stripped and probed with pan-Akt antibody for a loading control. *Lane 4* represents control C2C12 cells treated with 5 ng/ml TGFβ1. These experiments were repeated three times with similar results.

mouse dermal fibroblasts. As expected, mutant N-propeptide was also incapable of eliciting changes in phosphorylation. To test the possibility that one or more additional molecules, which were secreted by N-propeptide-expressing cells but absent from the purified protein, were required for the function of N-propeptide, conditioned medium from N-propeptide-expressing cells was added to COS-7 cells. Again, no changes in the phosphorylation levels of Akt or Smad3 were observed.

Externally added N-propeptide was also ineffective in altering the differentiation or synthetic capability of cells induced by BMP2 or TGFβ1. Thus, purified N-propeptide, despite its ability to interact with BMP2 as shown in Fig. 5*B*, did not inhibit the BMP2-induced differentiation of C2C12 cells when added externally (data not shown). This finding contrasts with the significant reduction in differentiation of stably transfected N-propeptide-expressing C2C12 cells, as compared with exon 2-deleted N-propeptide-expressing cells, when these cells were treated with BMP2 (Fig. 8*A*). N-propeptide also failed to inhibit the TGFβ1-induced synthesis and secretion of IL11 by A549 cells, a human adenocarcinoma cell line (data not shown).

DISCUSSION

In this study we demonstrate that endogenously acting recombinant, trimeric N-propeptide induces changes in protein phosphorylation in stably transfected COS-7 cells and inhibits the BMP2-induced differentiation of stably transfected C2C12 skeletal myoblasts to osteoblasts. COS-7 cells that express N-propeptide also have a significant reduction in the synthesis of type I collagen, attach poorly to fibronectin-coated plates, and are more readily detached by low concentrations of trypsin. However, the purified, recombinant N-propeptide, although capable of interacting with both TGFβ1 and BMP2, is unable to inhibit the physiological functions of these cytokines when added to the medium of cells in culture. All of the properties of the N-propeptide can be attributed to the CRD domain encoded by exon 2, because a recombinant N-propeptide that lacks this domain is inactive both in binding to cytokines and functionally. Furthermore, a mutation in N-propeptide that disrupts a conserved disulfide bond in the CRD (see below) also fails to signal in COS-7 cells. These findings suggest that the N-propeptide can function not only as an important feedback regulator of collagen synthesis but could also modulate other properties of cells that synthesize type I procollagen. Our finding that N-propeptide can inhibit collagen synthesis when the protein acts endogenously in COS-7 cells supports its previously suggested role as an important feedback regulator of collagen synthesis. The ability of N-propeptide to interact with TGFβ1 and BMP2 could also account for the significant level of fetal mortality in mice with a targeted deletion of exon 2 of the *Col1a1* gene (15), because the functions of members of the TGFβ superfamily are crucial during fetal development. However, the anatomical and biochemical basis for this mortality will require analyses of fetuses acquired by caesarian sections.

A surprising finding in this study is that the functional properties of endogenously acting N-propeptide are not reproduced when control cells are treated with purified N-propeptide. A possible explanation for this observation, namely that a secreted cofactor is required for the function of N-propeptide, is excluded by the inability of conditioned medium from COS-7-expressing cells to reproduce these effects when added to control COS-7 cells. It also seems unlikely that the procedure used for purification of N-propeptide (binding to and elution from an affinity column at 4 °C) could cause structural changes in the protein. Indeed, purified N-propeptide retains its ability to interact with TGFβ1 and BMP2. However, we cannot exclude the possibility that purified N-propeptide, or the conditioned medium from N-propeptide-expressing cells, will interact with cell-surface receptors on cells that have not yet been tested.

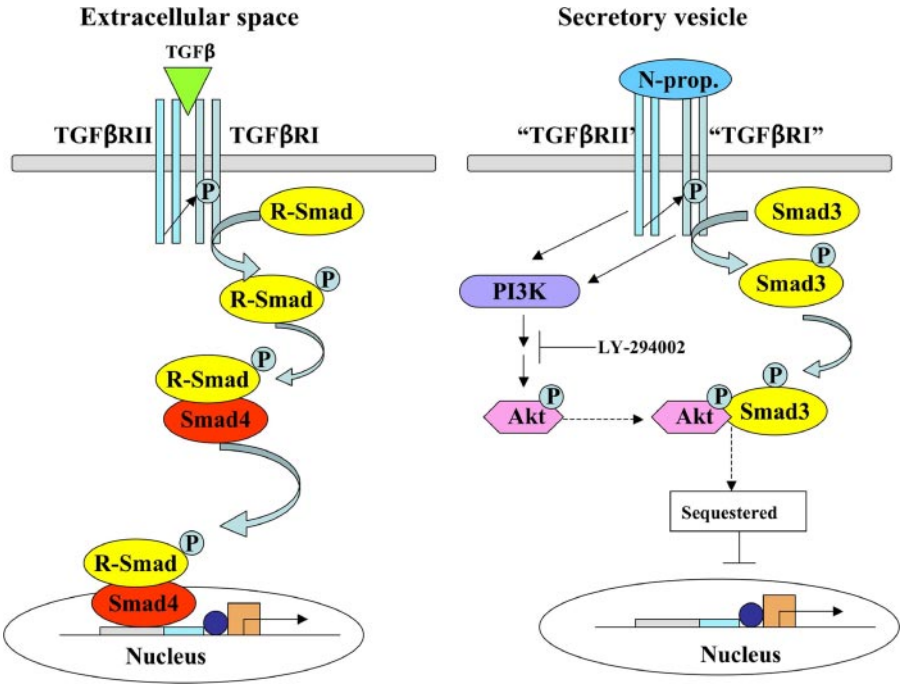

FIGURE 9. **A comparison of signaling pathways induced by the interaction of TGFβ1 with a TGFβR complex in plasma membranes with pathways induced by the interaction of N-propeptide with a TGFβR-like complex in secretory vesicle membranes.** The *left side* of the diagram depicts the classical TGFβR/Smad pathway. TGFβ1, which interacts initially with a betaglycan co-receptor, activates TGFβRII, which then dimerizes with and phosphorylates TGFβRI. Activated TGFβRI phosphorylates receptor Smad2 and Smad3 (*R-Smad-P*), which in turn interacts with mediator Smad4. The complex then translocates to the nucleus and activates the promoters of genes with appropriate cis-acting elements, such as *Col1a1*. The *right side* of the diagram shows a modified pathway that we propose accounts for the function of N-propeptide (*N-prop.*). N-propeptide interacts with a homologous bi-dimeric TGFβR-like complex, indicated by *quotation marks*, in secretory vesicle membranes. *"TGFβRI"* is capable of phosphorylating only Smad3. *"TGFβRI"* and *"TGFβRII"* independently activate PI3K, which in a complex series of steps phosphorylates Akt. We hypothesize that pAkt interacts with pSmad3 and that this complex is then hindered from entering the nucleus and activating transcription, perhaps because of sequestration. The *dashed arrows* indicate that the latter steps are hypothetical.

The Function of N-propeptide Requires the Native Structure of the CRD—The importance of the native structure of N-propeptide for its function is emphasized by the inability of the C52S mutant protein to cause changes in protein phosphorylation in COS-7 cells (Fig. 6, *A* and *B*). This mutation was patterned after a point mutation (nucleotide 182 G→C) detected in exon 2 in one allele of *COL1A1* in a young girl in whom a diagnosis of OI type I was made.[5] No other mutations in the two chains of type I procollagen were found. The mutation predicts the substitution of a serine for an evolutionarily conserved cysteine at amino acid 61 in the human protein. Although the three-dimensional structure of the type I procollagen N-propeptide is not known, the solution structure of the closely related human type II N-propeptide was published recently (29). This substitution would disrupt a disulfide bond and destabilize an anti-parallel β-sheet, which represents a major structural element in the N-propeptide. It is therefore almost certain that the mutation will cause major conformational changes in the N-propeptide.[6] These findings are important because they raise the possibility that some forms of OI could result from disturbances in effective levels of TGFβ1 or BMPs, rather than from a direct effect on collagen structure or levels of synthesis. An analogy can be made with recent findings that changes in TGFβ signaling are involved in some patients with the Marfan syndrome, who have mutations in TGFβR2 (30).

N-propeptide Functions Primarily Intracellularly—Is an intracellular mode of action for N-propeptide compatible with its status as an integral component of a secreted protein? Although it was widely believed that the proteolytic processing of the N- and C-propeptides of type I procollagen occurred only after secretion of the precursor, there is now good evidence that a significant fraction of the propeptides is released intracellularly in specialized secretory vesicles, termed Golgi to plasma membrane carriers (12, 31). These vesicles fuse with specialized regions of the plasma membrane, termed fibripositors, to deliver their cargo to the extracellular space (12). This trafficking pathway provides for the possibility of an intracellular mode of action for N-propeptide, although the mechanism by which this signal could be transduced is not known. Possibilities include interaction with a TGFβR-like receptor in secretory vesicles (Fig. 9) or access of the N-propeptide to the cytosol. Although it may seem unlikely that a secreted protein can also function intracellularly, there are now a number of well documented instances in which such dual functions have been demonstrated. Perhaps the closest parallel to the intracellular function of N-propeptide is that of the propeptide of lysyl oxidase. Lysyl oxidase is secreted as a proenzyme and is activated proteolytically to release an 18-kDa propeptide. The active enzyme oxidatively deaminates the ϵ-amino groups in lysyl and hydroxylysyl residues in collagen and elastin, the initial step in the formation of covalent cross-links in these proteins. However, the propeptide regains access to the cell and functions to inhibit *ras*-dependent transformation in fibroblasts (32). The authors hypothesize that the highly basic propeptide could permeate a lipid bilayer, but receptor-mediated uptake, or signaling via a membrane-bound receptor, has not been excluded.

An intracellular mode of action for N-propeptide raises the question of the physiological role for direct N-propeptide to cytokine interactions. One possibility relates to the well known sequestering function of the extracellular matrix. At least in cell culture, and possibly also *in vivo*, a fraction of type I procollagen escapes proteolytic conversion to collagen and is secreted as the intact precursor. Such molecules, with the N-propeptide covalently attached to a collagen helix, would be capable of

[5] J. M. Pace and P. H. Byers, personal communication.
[6] A. K. Downing, personal communication.

binding TGFβ1 and BMP2 and could serve as a storage compartment for these cytokines by binding to existing collagen fibrils. During matrix turnover, as might occur in wound healing, these cytokines could be released by collagenases to perform anabolic functions. An analogous sequence of events has been described for vascular endothelial growth factor (33).

N-propeptide Signals through a Modified TGFβ Receptor/Smad Pathway—Although our analysis of the signaling pathway activated by endogenously produced N-propeptide in COS-7 cells is not complete, there is sufficient information to suggest a mechanism by which collagen synthesis could be inhibited. Receptor-regulated phosphorylation of Smad2 and -3 leads to dimer formation with Smad4. Subsequently, these complexes are translocated to the nucleus and activate transcription of several Smad-responsive genes, including *Col1a1* (Fig. 9). Impairment of Smad complex formation will therefore result in a reduction of type I collagen gene expression (34).

There is a significantly increased level of the phosphorylated serine/threonine kinase Akt (pAkt) in N-propeptide-expressing COS-7 cells (Fig. 6*A*). The level of pSmad3 is also increased in these cells (Fig. 6*B*). Recent work has shown that in hepatic cells pAkt, induced by insulin, interacts directly with unphosphorylated Smad3 and that the resulting complex is sequestered in the cytoplasm and cell membranes, thus impairing the transcriptional activity of Smad3 complexes (35, 36). However, when phosphorylation of Smad3 is induced by TGFβ1, the interaction with pAkt has low affinity. In contrast, in N-propeptide-expressing fibroblast-like COS-7 cells, the levels of pAkt and pSmad3 are both elevated, and yet type I procollagen synthesis is markedly reduced. It is possible that in these cells pAkt-pSmad3 complexes retain a high affinity of binding, thus inhibiting the formation of Smad4-pSmad3 complexes and their nuclear translocation (Fig. 9). Alternatively, the inhibition of collagen synthesis by N-propeptide might not involve the Smad pathway in COS-7 cells.

It is known that increased levels of pSmad3 can be associated with apoptotic cell death (37). We therefore examined the survival of COS-7 cells expressing N-propeptide and found that the extent of apoptosis was not changed in these cells, compared with control cells. This finding is consistent with the presence of elevated levels of pAkt. Our observation that N-propeptide-expressing cells proliferate faster than control cells (data not shown) also supports the presence of a higher pAkt/pSmad3 ratio in these cells. It has been shown that pAkt, which is downstream of PI 3-kinase, is crucial for cell survival and that the ratio of pAkt to pSmad3 is an important factor in the regulation of cell survival (38). If this ratio favors pAkt, then pAkt could sequester Smad3, thus inhibiting apoptotic pathways and possibly other Smad3-specific pathways such as those leading to collagen synthesis.

Upon ligand binding, TGFβ type II serine/threonine kinase receptors phosphorylate and activate TGFβ type I receptors, which then signal to downstream targets, including Smad proteins. It has been shown that constitutively active TGFβRI can generate downstream signals without requiring a ligand or TGFβRII (39). We show here that Smad3 is activated in COS-7 cells that constitutively express N-propeptide (Fig. 6*B*). The levels of pAkt are also very high in these cells, even higher than the levels of pAkt in cells stimulated with TGFβ1 (Fig. 7). Our results also show that the TGFβRI kinase-specific inhibitor reduces the levels of pSmad3 to almost basal levels in N-propeptide-expressing cells, indicating that TGFβRI is activated in these cells (Fig. 7). The levels of activated Akt were also partially reduced, suggesting that Akt might be activated by both the TGFβRI and TGFβRII receptors. This possibility is supported by the observation that treatment of control COS-7 cells with TGFβ1 results in the activation of Akt (Fig. 7, *lanes 1* and *2*), which is not inhibited by the TGFβR1-specific inhibitor (Fig. 7, *lane 3*). Constitutive expression of N-propeptide in the mouse myoblast C2C12 cell line did not activate Smad2 or -3 but activated Akt (Fig. 8), suggesting that activation of receptors by N-propeptide is cell type-dependent. It is therefore possible that Akt is activated in N-propeptide-expressing C2C12 cells by receptors other than the TGFβR.

Both Smad2 and Smad3 are phosphorylated by activated TGFβ receptor kinases. Interestingly, we were not able to detect the activation of Smad2 in COS-7 cells expressing N-propeptide. The selectivity of activation of Smads, as observed in N-propeptide-expressing cells, most likely reflects differences in the mechanisms by which these proteins are activated. It has been shown that SARA (Smad anchor for receptor activation) and Hrs, two FYVE finger domain-containing proteins, cooperate to present Smad2 to TGFβRI for its activation (40, 41). However, SARA is not required for the activation of Smad3 (42). Therefore, the distinct interactions of SARA and Hrs may account for the differential activation of Smad2 and Smad3 proteins. Both SARA and Hrs are associated with the plasma membrane through their FYVE finger domains in the presence of phosphatidylinositol 3-phosphate, whose level is regulated by PI3K (40). Therefore, treatment of cells with the PI3K-specific inhibitor LY294002 is likely to deplete cellular stores of phosphatidylinositol 3-phosphate and thus block SARA-mediated activation of Smad2 and possibly Smad3. However, our data demonstrate that LY294002 did not reduce pSmad3 levels in N-propeptide-expressing cells (Fig. 6*C*, *lane 5*). Thus, SARA is not required for the activation of Smad3 in these cells. Our data therefore support the differential activation of Smad2 and Smad3 in N-propeptide-expressing COS-7 cells. It has also been shown that Smad2 and Smad3 are differentially activated in prostatic epithelial cells (43).

Our Data Support a Feedback Regulatory Function for N-propeptide—Our finding that mouse N-propeptide inhibits type I collagen synthesis supports the earliest investigation of the biological properties of this protein fragment. As described in the Introduction, Wiestner *et al.* (9) had shown that monomeric N-propeptide, derived from dermatosparactic calf pN-collagen, inhibited collagen synthesis by bovine and human fibroblasts, but no mechanism was proposed for its mode of action. Subsequently, studies from several laboratories suggested that monomeric N-propeptide might function to inhibit the translation of procollagen mRNA selectively (see Introduction). However, these findings raised the serious problem of how the N-propeptide could gain access to the cytosol, and no satisfactory resolution of this problem has been advanced. Although our data cannot be used to support the inhibition of translation of procollagen mRNA by N-propeptide, the intra-

cellular mode of action of our recombinant N-propeptide raises the possibility that an unusual receptor-mediated event could underlie its mechanism of action.

In our experiments, we have chosen to study the function of a recombinant homotrimeric $(\alpha1)_3$ form of the N-propeptide and to synthesize the protein in mammalian cells to preserve possible post-translational modifications. This choice was partly guided by expediency because a recombinant heterotrimeric N-propeptide $(\alpha1)_2\alpha2$, would be very difficult to produce, and natural sources of heterotrimeric N-propeptide, such as dermatosparactic pN-collagen, are not readily available. Furthermore, the use of a recombinant protein permitted the addition of His and Myc tags for purification and identification, respectively.

The Design of a Recombinant Homotrimeric N-propeptide Is Biologically Relevant—The prevalent form of the N-propeptide in adult mammalian tissues is the heterotrimeric form, which contains only two CRDs, because the proα2 chain lacks a sequence equivalent to that encoded by exon 2 in the *Col1a1* gene. However, a homotrimeric N-propeptide is physiologically relevant, because during embryonic development a homotrimeric protein, consisting of three identical α1 chains (termed α1 trimer), accounts for a significant proportion of type I collagen in some tissues (44–48). The special function of this variant form of type I collagen in development is not understood. It is possible that the interactive properties of α1 trimer with type I collagen-associated molecules, such as type V collagen and decorin, provide an advantage for type I collagen fibers that must be remodeled in a rapidly developing and growing embryo. An additional function for α1 trimer could be to serve as a source for a homotrimeric N-propeptide with three CRDs, which might be capable of binding TGFβ1 and BMPs more effectively than the corresponding N-propeptide with two CRDs that is released from heterotrimeric type I procollagen.

Evidence for the importance of multimerization of the CRD in the binding of BMP2 and BMP4 was first provided by the work of Larrain *et al.* (19). These authors showed that *Xenopus* chordin, which has four CRDs, two of which are high affinity-binding sites, has higher dorsalizing activity in embryo microinjection assays and binds BMP4 with dissociation constants that are 5–8-fold lower than any of the individual CRDs. It was proposed that intact chordin is required for optimal binding, although the results of combinations of individual CRDs were not reported. A model proposed by Larrain *et al.* (19) suggests that the two high affinity CRDs in chordin interact with a dimeric BMP4 molecule and that this complex prevents BMP4 from engaging the BMP receptor complex, with its resulting phosphorylation and activation of signaling. A similar model could be considered for the interaction of multimeric N-propeptide with TGFβ1, which also functions extracellularly as a dimer (49). The orientation of the two CRDs to each other in the heterotrimeric N-propeptide and the presence or absence of significant interactions between the two domains are not known. It is therefore possible that two of the three exon 2-encoded CRDs in α1 trimer are more favorably oriented to bind TGFβ1 than the two CRDs in the N-propeptide that is normally released from a heterotrimeric type I procollagen molecule.

An indication that a homotrimeric N-propeptide might be capable of binding cytokines more effectively than a heterotrimeric N-propeptide comes from a consideration of the phenotype of the *oim* mouse. The *oim* mouse is homozygous for a functionally null mutation in the *Col1a2* gene and therefore synthesizes homotrimeric type I procollagen exclusively (50). Lack of the α2 chain in this mouse results in reduced tensile strength of collagen-containing tissues such as skin, tendon, and aorta, and in altered biomechanical properties of bone (51). In addition, a reduced collagen content in bone (52), heart (53), and aorta (51) has been reported in *oim* mice and undoubtedly contributes to the compromised structural properties of these tissues. We suggest that more effective inhibition of TGFβ1 function by homotrimeric N-propeptide could contribute to the reduced collagen synthesis in these mice.

Although attention in the literature, and in this report, has focused on the NH_2-terminal globular domain, the N-propeptide also contains a highly conserved COOH-terminal domain that consists of a short triple helix. The physical properties of this triple helical domain were studied many years ago (54), but no consideration has since been given to its physiological significance. If one extrapolates from the data obtained for the type III N-propeptide (55), it is possible that the trimeric structure of the N-propeptide of heterotrimeric type I procollagen persists at body temperatures, because of the relatively high proline and hydroxyproline contents of the Gly-*X*-*Y* triplets that constitute the minor triple helix. In support of this conjecture, predictions of the thermal stability of a murine minor collagen triple helix composed of three α1 chains, in comparison with that generated by three α2 chains, strongly favor the homotrimeric α1 helix. This conclusion was reached by calculating the relative stability profiles of the two helices using the algorithm described by Persikov *et al.* (56). The algorithm is available on line. These considerations suggest that the synthesis of α1 trimer may be advantageous under conditions in which careful modulation of active cytokine levels is important. Thus, the relative prominence of α1 trimer during embryonic development, the nearly ubiquitous expression of type I procollagen in the developing fetus, and the functional properties of the N-propeptide, as described in this study, suggest an important role for the N-propeptide in morphogenetic events during development and growth, and later as a homeostatic agent.

In conclusion, we have shown that type I procollagen N-propeptide functions intracellularly in transfected COS-7 cells to cause changes in protein phosphorylation, a reduction in procollagen synthesis, and an impairment in cell adhesion. N-propeptide also binds TGFβ1 and BMP2 directly. Expression in myoblastic C2C12 cells inhibits differentiation to osteoblasts. Both the direct binding and functional effects of N-propeptide are entirely dependent on the CRD encoded by exon 2 of the *Col1a1* gene. This domain is homologous to the CRDs in proteins that play important morphogenetic roles in early development of both vertebrates and invertebrates. In view of the pleiotropic effects of TGFβ1 and the nearly ubiquitous synthesis of type I procollagen, the N-propeptide could play an important role in vertebrate development and homeostasis. Our results also suggest an important function for the minor triple helix in the N-propeptide in preserving the

multimeric structure of the N-propeptide following its proteolytic release from procollagen.

Acknowledgments—We thank Melanie Marohm for technical assistance, Drs. Barbara Brodsky and Anton Persikov (Robert Wood Johnson School of Medicine) for their assistance with calculations of the thermal stability of collagen helices, Martha Rapoza (Genzyme Corp.) for performing the A549 cell assays, and Dr. Peter Byers (University of Washington) for providing information regarding the human N-propeptide mutation prior to publication. Mouse myoblast C2C12 cells were a gift from Dr. S. Hauschka (University of Washington).

REFERENCES

1. Prockop, D. J., Sieron, A. L., and Li, S. W. (1998) *Matrix Biol.* **16,** 399–408
2. Doege, K. J., and Fessler, J. H. (1986) *J. Biol. Chem.* **261,** 8924–8935
3. Lees, J. F., Tasab, M., and Bulleid, N. J. (1997) *EMBO J.* **16,** 908–916
4. McLaughlin, S. H., and Bulleid, N. J. (1998) *Matrix Biol.* **16,** 369–377
5. Palmieri, D., Camardella, L., Ulivi, V., Guasco, G., and Manduca, P. (2000) *J. Biol. Chem.* **275,** 32658–32663
6. Palmieri, D., Poggi, S., Ulivi, V., Casartelli, G., and Manduca, P. (2003) *J. Biol. Chem.* **278,** 3639–3647
7. Katayama, K., Armendariz-Borunda, J., Raghow, R., Kang, A. H., and Seyer, J. M. (1993) *J. Biol. Chem.* **268,** 9941–9944
8. Bornstein, P. (2002) *Matrix Biol.* **21,** 217–226
9. Wiestner, M., Krieg, T., Hörlein, D., Glanville, R. W., Fietzek, P., and Muller, P. K. (1979) *J. Biol. Chem.* **254,** 7016–7023
10. Paglia, L., Wilczek, J., Diaz de Leon, L., Martin, G. R., Horlein, D., and Muller, P. (1979) *Biochemistry* **18,** 5030–5034
11. Hörlein, D., McPherson, J., Goh, S. H., and Bornstein, P. (1981) *Proc. Natl. Acad. Sci. U. S. A.* **78,** 6163–6167
12. Canty, E. G., Lu, Y., Meadows, R. S., Shaw, M. K., Holmes, D. F., and Kadler, K. E. (2004) *J. Cell Biol.* **165,** 553–563
13. Bornstein, P. (1974) *Annu. Rev. Biochem.* **43,** 567–603
14. Martin, G. R., Byers, P. H., and Piez, K. A. (1975) *Adv. Enzymol.* **42,** 167–191
15. Bornstein, P., Walsh, V., Tullis, J., Stainbrook, E., Bateman, J., and Hormuzdi, S. G. (2002) *J. Biol. Chem.* **277,** 2605–2613
16. Abreu, J. G., Coffinier, C., Larrain, J., Oelgeschläger, M., and deRobertis, E. M. (2002) *Gene* (*Amst.*) **287,** 39–47
17. deRobertis, E. M., Larrain, J., Oelgeschläger, M., and Wessely, O. (2000) *Nat. Rev. Genet.* **1,** 171–181
18. Holley, S. A., Neul, J. L., Attisano, L., Wrana, J. L., Sasai, Y., O'Connor, M. B., deRobertis, E. M., and Ferguson, E. L. (1996) *Cell* **86,** 607–617
19. Larrain, J., Bachiller, D., Lu, B., Agius, E., Piccolo, S., and deRobertis, E. M. (2000) *Development* (*Camb.*) **127,** 821–830
20. Piccolo, S., Sasai, Y., Lu, B., and deRobertis, E. M. (1996) *Cell* **86,** 589–598
21. Zhu, Y., Oganesian, A., Keene, D. R., and Sandell, L. J. (1999) *J. Cell Biol.* **144,** 1069–1080
22. Cheah, K. S. E., Wong, S. Y. Y., Zhang, J. C. L., Leung, A. W. L., Chan, D., and Tam, P. P. L. (2005) *Mech. Dev.* **122,** Suppl. 1, S25
23. Frank, S., Kammerer, R. A., Mechling, D., Schulthess, T., Landwehr, R., Bann, J., Guo, Y., Lustig, A., Bächinger, H. P., and Engel, J. (2001) *J. Mol. Biol.* **308,** 1081–1089
24. Hernandez-Canaveral, I., Gonzalez, J., Lopez-Castillas, F., and Armendez-Borunda, J. (2004) *J. Gastroenterol. Hepatol.* **19,** 380–387
25. Ignotz, R. A., and Massague, J. (1986) *J. Biol. Chem.* **261,** 4337–4345
26. Mauviel, A. (2005) *Methods Mol. Med.* **117,** 69–80
27. Chen, D., Zhao, M., and Mundy, G. R. (2004) *Growth Factors* **22,** 233–241
28. Yi, J. Y., Shin, I., and Arteaga, C. L. (2005) *J. Biol. Chem.* **280,** 10870–10876
29. O'Leary, J. M., Hamilton, J. M., Deane, C. M., Valeyev, N. V., Sandell, L. J., and Downing, A. K. (2004) *J. Biol. Chem.* **279,** 53857–53866
30. Neptune, E. R., Frischmeyer, P. A., Arking, D. E., Myers, L., Bunton, T. E., Gayraud, B., Ramirez, F., Sakai, L. Y., and Dietz, H. C. (2003) *Nat. Genet.* **33,** 407–411
31. Canty, E. G., and Kadler, K. E. (2005) *J. Cell Sci.* **118,** 1341–1353
32. Palamakumbura, A. H., Jeay, S., Guo, Y., Pischon, N., Sommer, P., Sonenschein, G. E., and Trackman, P. C. (2004) *J. Biol. Chem.* **279,** 40593–40600
33. Bergers, G., Brekken, R., McMahon, G., Vu, T. H., Itoh, T., Tamaki, K., Tanzawa, K., Thorpe, P., Itohara, S., Werb, Z., and Hanahan, D. (2000) *Nat. Cell Biol.* **2,** 737–744
34. Poncelet, A. C., and Schnaper, H. W. (2001) *J. Biol. Chem.* **276,** 6983–6992
35. Conery, A. R., Cao, Y., Thompson, E. A., Townsend, C. M., Jr., Ko, T. C., and Luo, K. (2004) *Nat. Cell Biol.* **6,** 366–372
36. Remy, I., Montmarquette, A., and Michnick, S. W. (2004) *Nat. Cell Biol.* **6,** 358–365
37. Sanchez-Capelo, A. (2005) *Cytokine Growth Factor Rev.* **16,** 15–34
38. Brazil, D. P., and Hemmings, B. A. (2001) *Trends Biochem. Sci.* **26,** 657–664
39. Wieser, R., Wrana, J. L., and Massague, J. (1995) *EMBO J.* **14,** 2199–2208
40. Miura, S., Takeshita, T., Asao, H., Kimura, Y., Murata, K., Sasaki, Y., Hanai, J. I., Beppu, H., Tsukazaki, T., Wrana, J. L., Miyazono, K., and Sugamura, K. (2000) *Mol. Cell. Biol.* **20,** 9346–9355
41. Tsukazaki, T., Chiang, T., Davison, A., Attisano, L., and Wrana, J. (1998) *Cell* **95,** 779–791
42. Goto, D., Nakajima, H., Mori, Y., Kurasawa, K., Kitamura, N., and Iwamoto, I. (2001) *Biochem. Biophys. Res. Commun.* **28,** 1100–1105
43. Song, K., Cornelius, S. C., Reiss, M., and Danielpour, D. (2003) *J. Biol. Chem.* **278,** 38342–38351
44. Crouch, E., and Bornstein, P. (1978) *Biochemistry* **17,** 5499–5509
45. Haralson, M. A., Jacobson, H. R., and Hoover, R. L. (1987) *Lab. Investig.* **57,** 513–523
46. Jimenez, S. A., Bashey, R. I., Benditt, M., and Yankowski, R. (1977) *Biochem. Biophys. Res. Commun.* **78,** 1354–1361
47. Nakamura, T., and Nagai, Y. (1980) *J. Biochem.* (*Tokyo*) **87,** 629–637
48. Shupp-Byrne, D. E., and Church, R. L. (1982) *Collagen. Relat. Res.* **2,** 481–494
49. Murphy-Ullrich, J. E., and Poczatek, M. (2000) *Cytokine Growth Factor Rev.* **11,** 59–69
50. Chipman, S. D., Sweet, H. O., McBride, D. J., Jr., Davisson, M. T., Marks, S. C., Jr., Shuldiner, A. R., Wenstrup, R. J., Rowe, D. W., and Shapiro, J. R. (1993) *Proc. Natl. Acad. Sci. U. S. A.* **90,** 1701–1705
51. Pfeiffer, B. J., Franklin, C. L., Hsieh, F., Bank, R. A., and Phillips, C. L. (2005) *Matrix Biol.* **24,** 451–458
52. Camacho, N. P., Hou, L., Toledano, T., RIlg, W. A., Brayton, C. F., Raggio, C. L., Root, L., and Boskey, A. L. (1999) *J. Bone Miner. Res.* **14,** 264–272
53. Weis, S. M., Emery, J. L., Becker, K. D., McBride, D. J., Jr., Omens, J. H., and McCullock, A. D. (2000) *Circ. Res.* **87,** 663–669
54. Engel, J., Bruckner, P., Becker, U., Timpl, R., and Rutschmann, B. (1977) *Biochemistry* **16,** 4026–4033
55. Bruckner, P., Bachinger, H. P., Timpl, R., and Engel, J. (1978) *Eur. J. Biochem.* **90,** 595–603
56. Persikov, A. V., Ramshaw, J. A. M., and Brodsky, B. (2005) *J. Biol. Chem.* **280,** 19343–19349